Spin-symmetry broken ground-state of UO₂ in DFT+U approach: the SMC method

M Payami

School of Physics and Accelerators, Nuclear Science and Technology Research Institute, AEOI, P.O. Box 14395-836, Tehran, Iran

E-mail: Mpayami@aeoi.org.ir

Abstract

It turns out that the ground states of some systems are symmetry-broken states in which some property is not symmetrically distributed. In the case of strongly correlated electron systems that were studied by the DFT+U method, researchers have shown that the total energy of the system is a multi-minima function of electron-configuration parameters and one has to single out the ground state out of the couples of minimum-energy states. However, the methods already introduced to determine these local minimum states, were not able to predict all such states, which may include the "true" ground state. In this work, we introduce a new simple and straight-forward method of SMC to find the GS as well as the meta-stable states of the 1k-order anti-ferromagnetic configuration for UO₂. Using this method, it is shown that the ground state of the UO₂ system is a spin-symmetry broken state of the electron spin magnetizations of oxygen atoms. Depending on the way we apply the SMC method, we obtain different numbers of meta-stable states, but the same ground states. The energetic properties, geometric properties, the electronic density distributions, and the electronic polarization density distributions of the ground state and the meta-stable states are shown to be different from each other. These properties also are shown to be sensitive to the magnitude of the initial opposite magnetizations of up-spin U-atoms (U1) and down-spin U-atoms (U2) in the 1k-order anti-ferromagnetic configuration, but the number of meta-stable states as well as the ground-state properties are insensitive to this magnitude. Using the PBEsol-GGA approximation for the exchange-correlation, we obtain the ground-state properties in excellent agreement with experiments.

Keywords: uranium dioxide, density-functional theory, anti-ferromagnetism, strongly-correlated system, meta-stable state

1. Introduction

UO₂ is one of the common fuels used in nuclear power reactors. The experimental studies have shown that UO₂ has an anti-ferromagnetic (AFM) crystal structure with a 3k-order at temperatures less than 30 K, while it assumes a paramagnetic form at higher temperatures [1,2]. In the low-temperature structure, as shown [3] in fig. 1, the uranium atoms occupy the sites of an FCC crystal structure with a lattice constant of 5.47 Angstrom and the oxygen atoms occupy positions with $Pa\bar{3}$ symmetry [4].

The electronic structure of UO₂ has already been investigated by other researchers [5-14]. It is well-known that the ordinary approximations used in density-functional theory (DFT) [15-16] description of the system usually lead to incorrect metallic behavior while it is experimentally found to be an insulator, the so-called "Mott insulator". The incorrect metallic prediction arises from the usual approximations in which the partially-filled "localized" *5f* and *6d* valence electrons in uranium atoms are treated on the same footing as other "delocalized" ones in the atom. To overcome this problem, one of the ways researchers commonly resort to, is the method of DFT+U [11,17-19] which is also adopted here in our calculations; another method (which is computationally very expensive) is using orbital-dependent hybrid functionals for the exchange-correlation (XC) energy functional [13, 35].

It has already been noticed that in the DFT+U method, the total energy of the system behaves as a
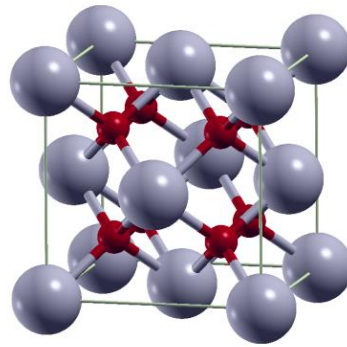
Figure 1. UO₂ crystal structure at low temperatures. The U atoms occupy the FCC lattice sites while the oxygen atoms adopt positions with $Pa\bar{3}$ symmetry having an experimental lattice constant equal to 5.47 Angstrom.

multi-minima function of electron-configuration parameters [11, 19-20]. To avoid the non-ground-state energy minima, the so-called "meta-stable" states (MS), researchers usually resort to the methods of occupation-matrix control [11], simulated-annealing [21], and U-ramping [22]. Each of those methods may help one to find lower-energy states but no guarantee of being the lowest-energy state, i. e., the "true" ground state (GS). In this work, we introduce a new simple and straight-forward method of "starting-magnetization control" (SMC) to find the true GS as well as the meta-stable states of 1k-order AFM UO₂. Using this method, it is shown that the true GS of the UO₂ system is a spin-symmetry broken state of the electron spin magnetizations of oxygen atoms.

In the SMC method, one scans different starting magnetizations for the two types of oxygen atoms in the interval [-1,+1] with reasonable steps, while the starting magnetizations for the two types of uranium atoms are kept fixed at +0.5 and -0.5. It is shown that using this method in the self-consistent (SCF) solution of the spin-polarized Kohn-Sham (KS) equations [16], the system converges to the nearest local minimum, which is one of the meta-stable states or the true GS (From now on for simplicity we omit "true" in the text.). Then, one singles out the sub-intervals that lead to the global minimum, i.e., the ground-state, and uses them in the further calculations of the ground-state properties.

Examining different XC schemes, we found that the generalized gradient approximation (GGA-PBEsol) [23] results in the best agreement with the experimental lattice constant and KS electronic band-gap. Therefore, in the calculations of this work we employ GGA-PBEsol. In the second step, we apply the SMC method to single out the appropriate sub-intervals for the starting magnetization and stick to them for further calculations of ground-state properties of UO₂. In all our calculations, the simplified model of 1k-order AFM configuration for uranium atoms was used. The results for the GS show excellent agreement with the experimental lattice constant and electronic band gap.

The organization of this paper is as follows. In Section 2, the computational details are presented; in Section 3 the calculated results are presented and discussed; Finally, Section 4 concludes this work.

2. Computational Details
All calculations are based on the solution of the KS equations in DFT using the Quantum-ESPRESSO code package [24, 25]. For the atoms U and O, we have employed the ultra-soft pseudo-potentials (USPP) generated by the *atomic* code, using the generation inputs (with small modifications for more accurate results) from the *pslibrary* [26], at https://github.com/dalcorso/pslibrary.

For the USPP generation, we have used the valence configurations of U($6s^2$, $6p^6$, $7s^2$, $7p^0$, $6d^1$, $5f^3$) and O($2s^2$, $2p^4$); and to take into account the relativistic effects of the electrons, we have adopted the scalar-relativistic method [27]. In another work, the authors have shown [28] that for studying the geometric properties it is necessary to go beyond and consider the full-relativistic method, which includes the spin-orbit effects.

Performing convergency tests, the appropriate kinetic energy cutoffs for the plane-wave expansions were chosen as 90 and 720 Ry for the wavefunctions and densities, respectively. To avoid the self-consistency problems, we have used the Methfessel-Paxton smearing method [29] for occupations with a width of 0.01 Ry. For the Brillouin-zone integrations in geometry optimizations, a 6×6×6 grid with a shift was used; while for density-of-states (DOS) calculations, we have used a denser grid of 8×8×8 in reciprocal space and the "tetrahedron" method [30] for the occupations. In DFT+U calculations, we have used the optimum value of 4.0 eV for the Hubbard-U parameter for the localized *5f* electrons of an uranium atom, consistent with the values determined by other works [31, 32]. All geometries were fully optimized for total pressures on unit cells to within 0.5 kbar, and forces on atoms to within 10^{-6} Ry/a.u.

To apply the SMC method to find the meta-stable states as well as the GS, we keep fixed the starting magnetizations of U1 and U2 atoms at +0.5 and -0.5, respectively; and change the values for O atoms in the interval [-1,+1] with steps of 0.1. To this end, we have first considered one and the same degrees of freedom for the starting magnetization of all oxygen atoms in the unit cell, and after optimization of the structures, obtained sixteen different local-minimum energy states (some of them doubly-degenerate) including the GS. However, the

Table 1. Equilibrium lattice constants in Angstrom, total and absolute magnetizations in Bohr-magneton per unit formula, and the electronic band gap in eV, using the PBEsol for the XC.

a (c)	a (Exp.)	Tot. mag.	Abs. mag.	E_g
5.5086 (5.4796)	5.470	0.00	2.165	2.10
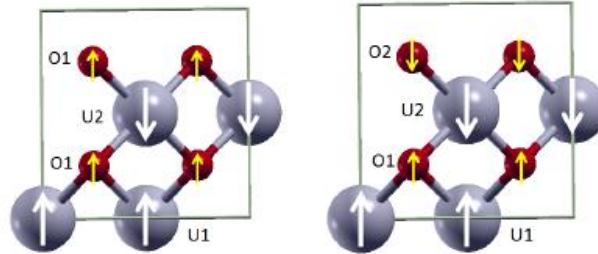
Figure 2. All-equivalent oxygen atoms scheme (left) and two-inequivalent oxygen atoms scheme (right). In the all-equivalent oxygen atoms model, all oxygen atoms are treated as the same type, O1, and assume the same starting magnetizations within the SMC method; while in two-inequivalent oxygen atoms model, the O1 and O2 oxygen atoms are treated as different types and assume independent values for the starting magnetizations in the SMC method.

spin-alignments of uranium atoms in the 1k-order AFM configuration imply that the oxygen atoms in the planes near to the planes of uranium atoms with different spin-alignments may behave independently. We have therefore released the constraint of all-equivalent oxygen atoms, and treated the oxygen atoms near to inequivalent uranium atoms as inequivalent ones. In this way, we have tried different starting magnetizations for the two types of oxygen atoms separately, while the starting magnetizations for the two types of uranium atoms were kept fixed at +0.5 and -0.5. Consequently, the optimization of the structures leads to more meta-stable states compared to all-equivalent oxygen atoms treatment. To assure not missing any meta-stable state due to possible inappropriate magnetization steps, we have reduced the step size from 0.1 to 0.05 and did not find any new states.

3. Results and Discussions
To make our calculation results in the most agreement with experiments, we first choose the best XC which results in the lattice constant and the electronic band-gap closest to the experimental one. Due to modeling the low-temperature system with a 1k-order AFM, the lattice constant along z direction becomes slightly different from that in a perpendicular direction. Using DFT+U and choosing Hubbard parameter U=4.0 eV, we have obtained the best values for the equilibrium lattice constants and the electronic band-gap using the PBEsol, and the result is shown in table 1. In all subsequent calculations we use this XC functional.

3. 1. Determining meta-stable states using the SMC method
3. 1. 1 All-equivalent O-atoms
As was mentioned earlier, we first consider three types of atoms in the cell, as shown in fig. 2. In this model, all oxygen atoms are treated as the same type and assume the same starting magnetization within the SMC method. In this model, the spin-polarized KS equations were

solved for all possible starting magnetizations for the O atoms, while those for U atoms were kept fixed at +0.5 and -0.5. It should be mentioned that the magnetization for an atom with respective $N_\uparrow$ and $N_\downarrow$ spin-up and spin-down valence electrons is given by $\zeta = (N_\uparrow - N_\downarrow)/(N_\uparrow + N_\downarrow)$ which varies between -1 and +1. The geometries were fully optimized for each value of the starting magnetization of the O1 atom. The results show seven different classes of energetic and structural properties which are summarized in table 2. The calculated total magnetizations $M_{tot} = \int_{cell} (n_\uparrow - n_\downarrow) d^3r$ and absolute magnetizations $M_{abs} = \int_{cell} |n_\uparrow - n_\downarrow| d^3r$ show that the GS as well as most of meta-stable states have zero total magnetizations. The $n_\uparrow$ and $n_\downarrow$ are the spin-up and spin-down electron densities, respectively. To continue calculations for the GS, one simply uses the initial magnetization giving rise to the GS energy.

To make the situation clearer, we have schematically shown in fig. 3 how each starting magnetization leads to the corresponding local minimum.

As is shown in fig. 3, considering small values for the starting magnetization, in order to break the symmetry between spin-up and spin-down polarization in a spin-polarized calculation with DFT+U, does not necessarily lead to the GS.

3. 1. 2 Two inequivalent O-atoms
In this generalization, we distinguish four types of atoms in the unit cell, as shown in fig. 2: U1(0.00), U2(0.50), O1(0.25), and O2(0.75), where the values within parentheses specify the z-components of atomic positions in units of a=5.47 Angstrom, before geometry optimization.

Table 2. GS and meta-stable states' properties in the simplified all-equivalent oxygen atom model. The energies are in Ry/(unit formula) and are compared to the GS. Equilibrium lattice constants are in Angstrom, total and absolute magnetizations are in Bohr-magneton/(unit formula). GS, M2, and M3 are doubly degenerate states.

State	ΔE	a (c)	Tot. mag.	Abs. mag.
GS	0.0000	5.5086 (5.4796)	-0.00	2.165
GS′	0.0000	5.5086 (5.4796)	+0.00	2.165
M1	0.0027	5.5219 (5.4562)	±0.00	2.155
M2	0.0118	5.5299 (5.4396)	-0.00	2.165
M2′	0.0118	5.5299 (5.4396)	+0.00	2.165
M3	0.0588	5.4690 (5.5103)	-0.04	2.240
M3′	0.0588	5.4690 (5.5103)	+0.04	2.240
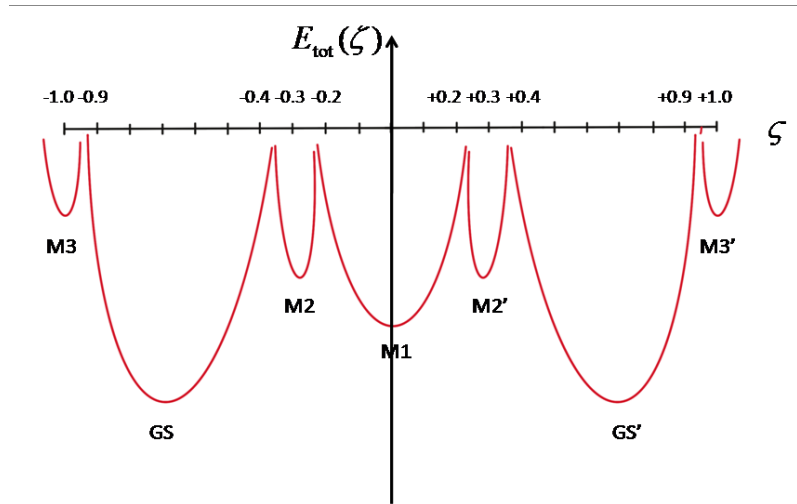
Figure 3. Schematic plot of local minima and their corresponding starting magnetizations. The depths of the minima (in arbitrary units) are consistent with their energy values. As is seen, the GS and GS' cover the largest interval, but away from the zero starting magnetization.

To apply the SMC method to find the meta-stable states as well as the GS, we keep fixed the starting magnetizations of U1 and U2 atoms at +0.5 and -0.5, respectively, as before; and change the values for O1 and O2 atoms independently, in the interval [-1, +1] with steps of 0.1. Then, for each pair of initial magnetizations ζ_1 and ζ_2, we perform a structural optimization as explained in the previous subsection. In this case, we obtained the GS and 16 meta-stable states with energies within 0.0588 Ry/(unit formula) above the GS. Our results show that the number of meta-stable states is about two times larger than the number of states reported in other previous works [11,14]. As shown in fig. 3 corresponding to the simplified model, some meta-stable states cover larger starting-magnetization interval than others. For example, the GS covers the interval $\zeta \in [-0.9, -0.4]$ and the GS' covers $\zeta \in [+0.4, +0.9]$, so that the total occurrences for the lowest-energy state is 12 out of a total 21 different ζ values in the interval [-1.0,+1.0]. We therefore include, in the generalized case, the occurrences of the states as well. Here we have named the meta-stable states as "MS" to distinguish them from those of the simplified model, "M". As is seen, the states obtained in the simplified model are also included in the generalized case but with different naming.

In table 3, the results for local-minima states of the generalized case are summarized. In this generalized case of two inequivalent O1 and O2 atoms, we have totally 21×21=441 different pairs of (ζ_1, ζ_2) values. 7 cases did not converge, and so the sum of occurrences in table 3 amounts to 434 cases. As is seen, the meta-stable states of M1, M2, and M3 in the simplified model are reappeared as MS1, MS3, and MS16 in the generalized model. Here, also as in the simplified model, the small values for both starting magnetizations do not converge to the GS.

3. 2. Properties of the GS and MS's
In this section, we compare the electronic structure properties of the GS with those of M1, M2, and M3, as defined in the simplified model.

3. 2. 1. Density of states (DOS)
In fig. 4, the spin-up and spin-down density of states for the ground state GS and meta-stable states M1, M2, and M3 are compared. As is seen, the first three states GS, M1, and M2 are insulators, with electronic gaps of 2.10, 2.10, and 1.70 eV, respectively; while the meta-stable

Table 3. GS and meta-stable states' properties in the two-inequivalent O1 and O2 model. The energies are in Ry/(unit formula) and are compared to the GS. Equilibrium lattice constants are in Angstrom, total and absolute magnetizations are in Bohr-magneton/(unit formula).

| State	ΔE	A (c)	Tot. mag.	Abs. mag.	Occ.
GS	0.00000	5.5086 (5.4796)	0.00	2.165	187
MS1	0.00275	5.5219 (5.4562)	0.00	2.155	117
MS2	0.00539	5.5040 (5.4835)	0.00	2.155	6
MS3	0.01184	5.5299 (5.4396)	0.00	2.165	53
MS4	0.02889	5.4803 (5.5020)	0.00	2.240	5
MS5	0.02893	5.4855 (5.4861)	0.00	2.240	3
MS6	0.03008	5.5054 (5.4740)	0.00	2.180	4
MS7	0.03040	5.4939 (5.4738)	0.00	2.240	17
MS8	0.03046	5.4848 (5.4932)	0.00	2.245	7
MS9	0.03176	5.4851 (5.4874)	0.00	2.235	1
MS10	0.03186	5.4848 (5.4932)	0.00	2.205	1
MS11	0.03192	5.4842 (5.4637)	0.00	2.230	1
MS12	0.05764	5.4657 (5.4895)	0.00	2.300	25
MS13	0.05767	5.4746 (5.4749)	0.00	2.300	1
MS14	0.5774	5.4701 (5.4829)	-0.025	2.300	2
MS15	0.05790	5.4647 (5.4433)	0.00	2.290	2
MS16	0.05879	5.4690 (5.5103)	±0.04	2.240	2
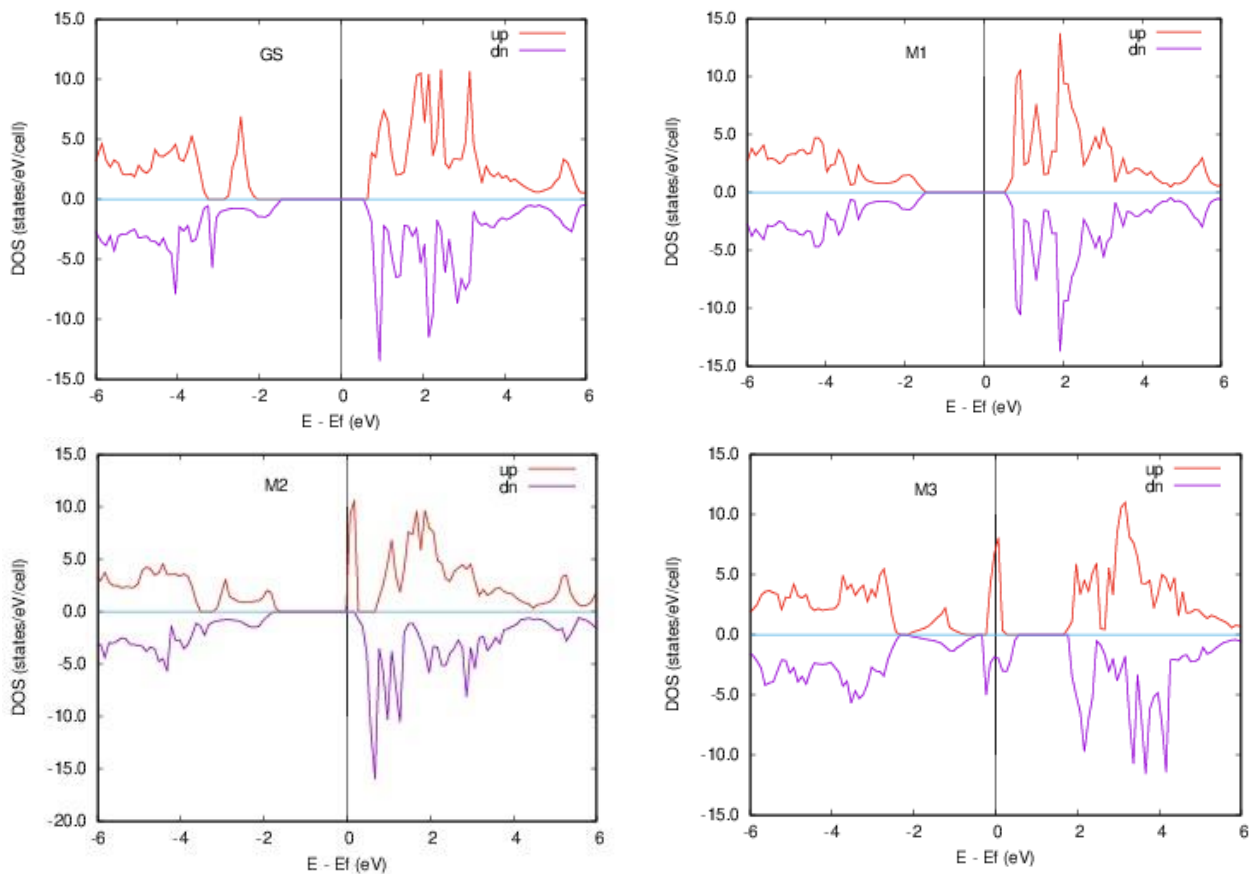
Figure 4. Spin-up and spin-down density of states for the GS and meta-stable states M1, M2, M3. The first three ones GS, M1, M2 are insulators, while M3 shows metallic behavior.

state M3 shows a narrow-band metallic behavior. The small gap in the valence band around 3.0 eV below the Fermi level for the spin-up GS comes from the uranium *5f* orbitals, as will be seen from the projected density of states (PDOS) in the following. A similar small gap is also observed in the conduction band of meta-stable state M2 around 0.5 eV above the Fermi level for spin-up.

In fig. 5, the spin-up and spin-down electronic band
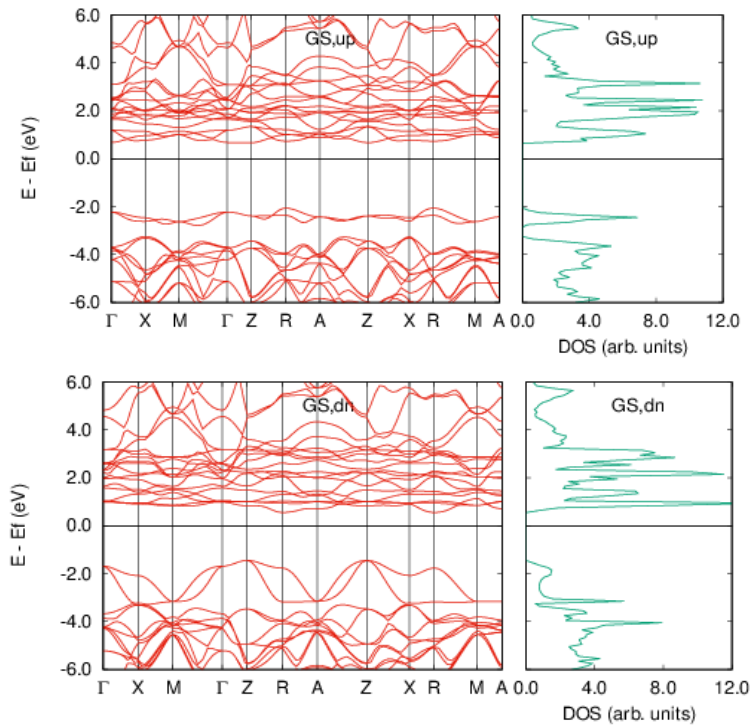
**Figure 5.** Spin-up and spin-down density of states and their corresponding band structures for the GS.
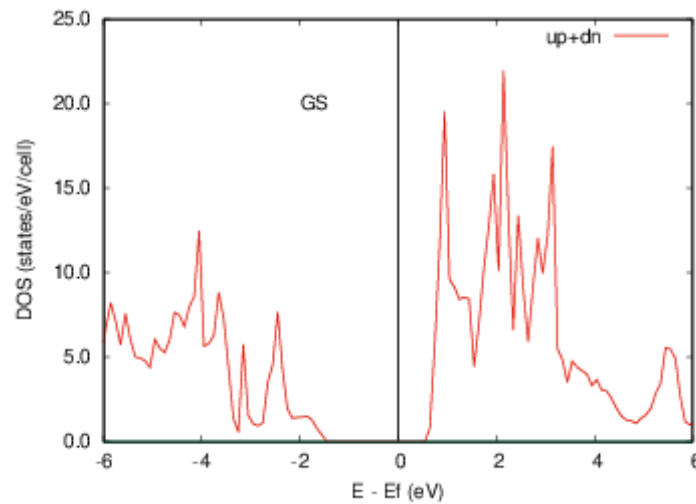
Figure 6. Total DOS for the GS. The small gap of spin-up as shown in fig. 5 is disappeared. The electronic band gap is determined from the total-DOS to be 2.10 eV.

structures with their corresponding density of states for the GS are shown. To calculate the band structures, we have used the appropriate k-point pathway [33, 34] of Γ - X - M - Γ - Z - R - A - Z - X - R - M - A. As was discussed earlier, the small band-gap in the spin-up is also present in the corresponding band structure. The narrow valence band of spin-up around 2.0 eV below the Fermi level originates from the uranium *5f* orbitals. The valence band-edge here, however, is determined by the spin-down states and the small gap is not present in the total density of the states plot, as shown in fig. 6. The electronic band gap is determined by the total-DOS which is 2.10 eV for the GS.

3. 2 .2. Projected density of states (PDOS)

To analyze the contributions of each valence atomic orbital to the density of states, we use the projections of wavefunctions over atomic orbitals, and then calculate DOS projected onto atomic orbitals, named PDOS. Here, we have plotted the contributions of five valence atomic orbitals *6s, 6p, 7s, 6d, 5f* of U-atoms and the two valence atomic orbitals *2s, 2p* of O-atoms for all states GS, M1, M2, and M3.

It is seen from fig. 7 that the *5f* orbitals have the strongest contribution in the density of states of both valence and conduction bands in all GS, M1, M2, and M3. This fact is clear from the different ranges of values of PDOS for different orbitals.
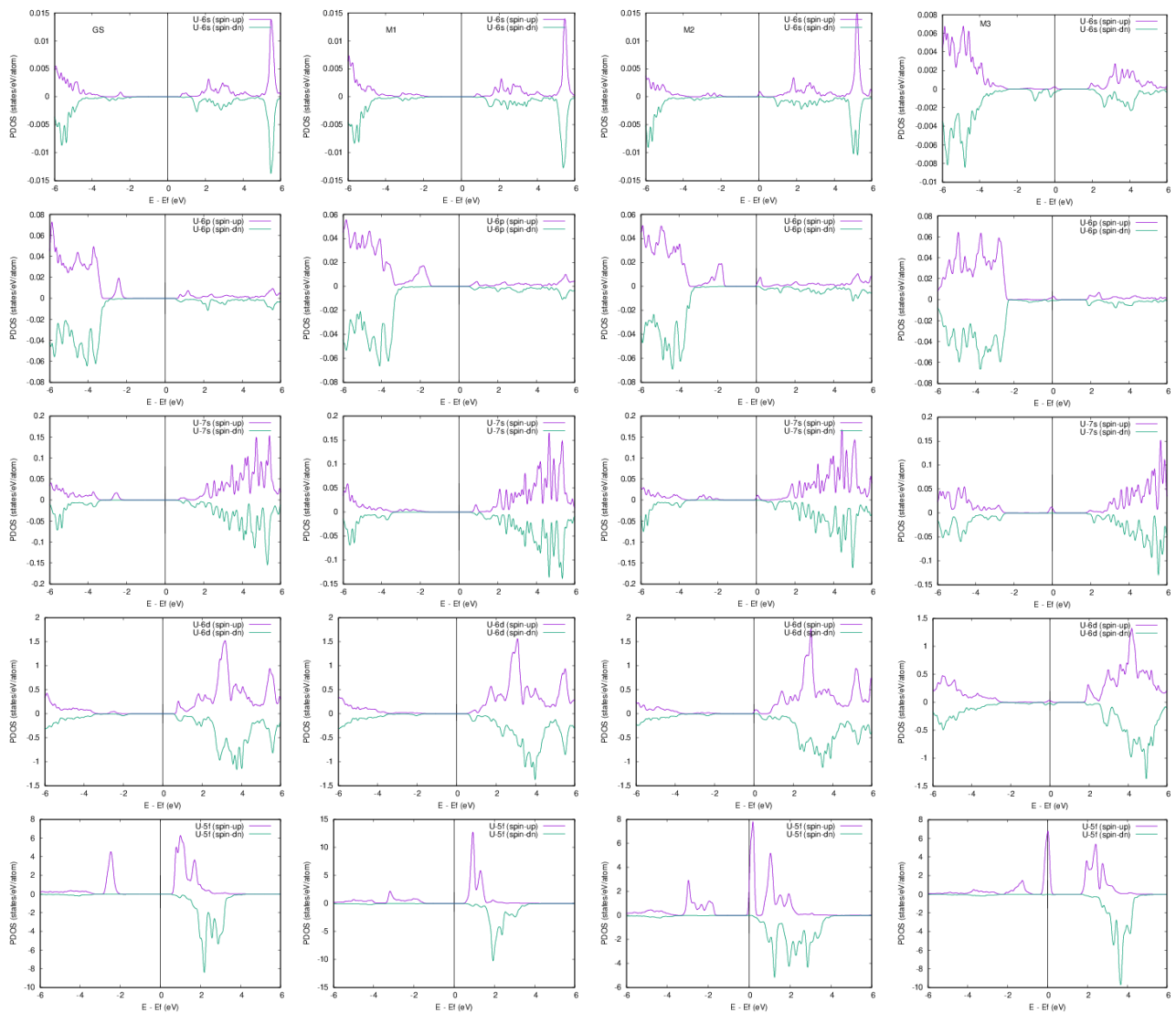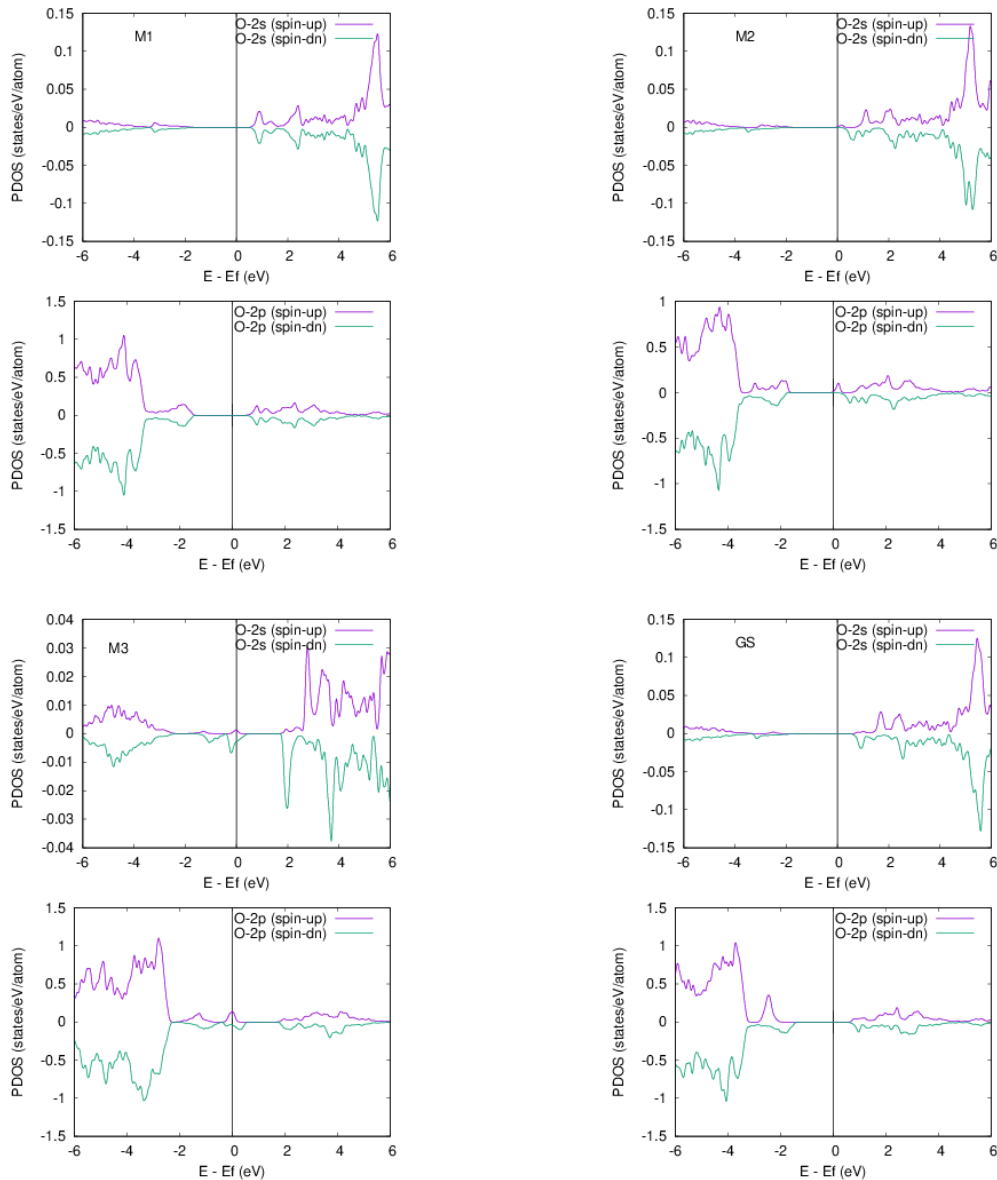
Figure 7. Projected density of states onto five atomic valence atomic orbitals *6s, 6p, 7s, 6d, 5f* of U-atoms. From different ranges of values of different orbitals' PDOS, it is seen that the *5f* orbitals have the strongest contribution in the density of states of both valence and conduction bands in all GS, M1, M2, and M3. None of the atomic orbitals have contributions to DOS of GS, M1, and M2 states at the Fermi level, and therefore, these three states show insulating behaviors. However, in M3 all atomic orbitals have contributions to DOS at Fermi level, and so this state has metallic behavior.

It is seen that the spin-down contributions of *5f* in the valence band are negligible compared to those of spin-up for all states. The contributions of *6d* are almost similar for the spin-up and spin-down. The strength of *6d* orbitals are smaller than those of *5f*, but of the same order. On the other hand, the strength of *7s* orbitals are one order of magnitude smaller than those of *5f* and *6d*. The strengths of *6p* and *6s* are two and three orders of magnitude smaller than *5f*, respectively. None of the atomic orbitals show any contributions to DOS of GS, M1, and M2 states at the Fermi level, and therefore, these three states have insulating behaviors. However, it is seen from fig. 7 that in M3 all atomic orbitals have contributions to DOS at Fermi level, and so this state has metallic behavior.

In fig. 8, we have plotted the contributions of two valence atomic orbitals *2s* and *2p* of O-atoms for all states GS, M1, M2, and M3. As is seen, the *2p* orbitals

have one order of magnitude stronger contributions in DOS than the *2s* ones of both valence and conduction bands in all GS, M1, M2, and M3. Here also, as in the case of U-atoms, none of the atomic orbitals have contributions to DOS of GS, M1, and M2 states at the Fermi level, and therefore, these three states show insulating behaviors. However, in M3 both *2s* and *2p* atomic orbitals have contributions to DOS at Fermi level, and so this state has metallic behavior. Comparing the PDOS's of O-atoms for GS and M1 we see an important difference. As we observed from fig. 3, the M1 state is achieved when we used small starting magnetizations around zero; therefore, the spin-up and spin-down contributions are similar, which is obtained when we constrain the starting magnetization to zero value. That is, we have symmetry between the spin-up and spin-down contributions for the O-atoms in M1.

In fig. 9, the local electronic polarizations

Figure 8. Projected density of states onto two atomic valence atomic orbitals *2s* and *2p* of O-atoms. The *2p* orbitals have one order of magnitude stronger contributions in DOS than the *2s* ones of both valence and conduction bands in all GS, M1, M2, and M3. Here also, as in the case of U-atoms, none of the atomic orbitals have contributions to DOS of GS, M1, and M2 states at the Fermi level, and therefore, these three states show insulating behaviors. However, in M3 both *2s* and *2p* atomic orbitals have contributions to DOS at Fermi level, and so this state has metallic behavior.

$(n_\uparrow(r) - n_\downarrow(r)) / (n_\uparrow(r) + n_\downarrow(r))$ for the GS and the meta-stable states are shown.

Finally, to check the dependence of the energetic and geometric properties of the GS as well as the meta-stable states on the values of the starting magnetizations ± 0.5 for the U1 and U2 uranium atoms in the 1k-order AFM configuration, we have set the starting magnetizations of U1 and U2 atoms to +1.0 and -1.0 respectively, and repeated the simplified all-equivalent oxygen atoms model calculations. The results are summarized in table 4.

To distinguish between these states from the previous ones, we have named them as GS*, M1*, M2*, M3*, M4*, M5*, and M6*. The first important message of the results in table 4 is that the energetic and geometric behaviors of the meta-stable states strongly depend on

the initial magnetization of the U-atoms. The second important result is that the degeneracies in the meta-stable states were disappeared and all new meta-stable states have different geometric properties, while the magnetization properties may still have similar properties. The third and final finding is that in all the three studied schemes, we obtained one and unique GS properties.

4. Conclusions

In this work, it was shown that within the SMC method, the "true" GS of the 1k-order AFM UO_2 system is a spin-symmetry broken state of the electron spin magnetization of oxygen atoms. In the DFT+U approach for strongly correlated systems, the total energy of the system is a multi-minima function of electron-
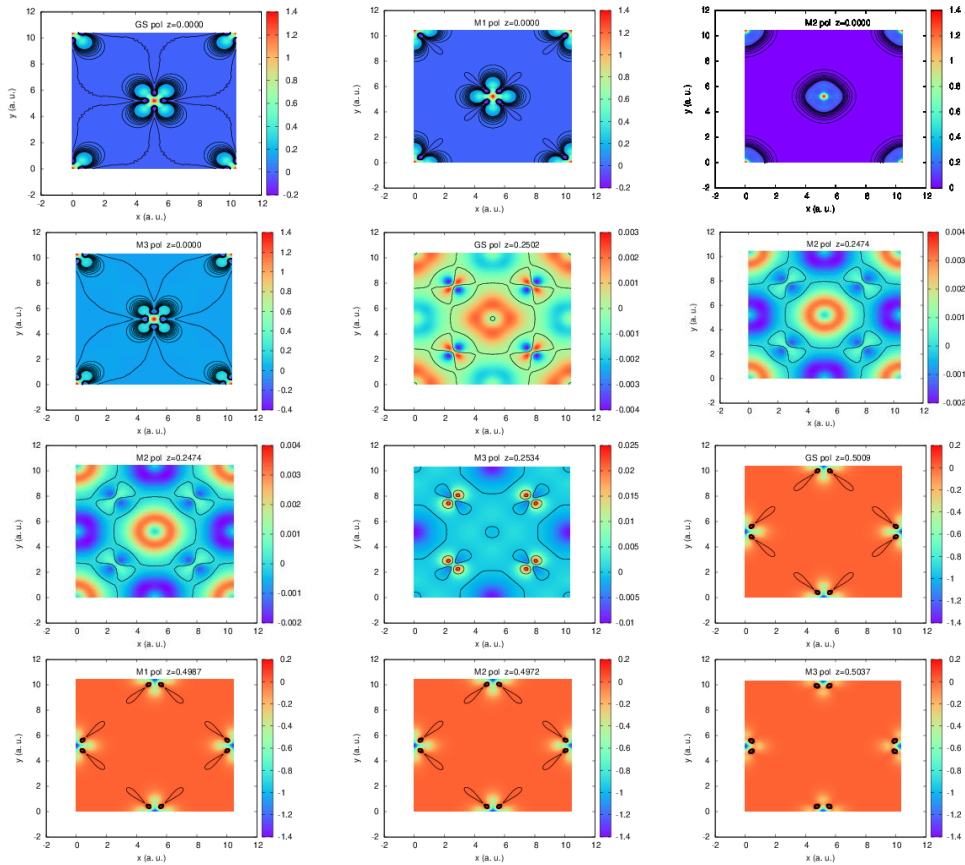
Figure 9. Local electronic polarization densities, $(n_\uparrow(r) - n_\downarrow(r)) / (n_\uparrow(r) + n_\downarrow(r))$, in atomic units, at equilibrium positions of the planes with z_1, z_2, and z_3 values for GS, M1, M2, and M3 states. As written in the sub-figures, the z-values are different for the GS, M1, M2, and M3 states. The z_1 planes contain the uranium atoms with up-spin configuration in the unit cell. The z_2 planes pass through the oxygen atoms of the unit cell, and the z_3 planes contain the second type of uranium atoms with down-spin configurations in the AFM structure. The values of the first three states at z_3 planes show similar behaviors which are different from that of the M3 state, which has metallic behavior.

Table 4. GS and meta-stable states' properties in the simplified all-equivalent oxygen atom model for the case of ± 1.0 initial magnetizations for U-atoms. The energies are in Ry/(unit formula) and are compared to the GS. Equilibrium lattice constants are in Angstrom, total and absolute magnetizations are in Bohr-magneton/(unit formula). GS*, M1*, M2*, M3*, M4*, M5*, and M6* states are different from each other.

State	ΔE	a (c)	Tot. mag.	Abs. mag.	Occ.
GS*	0.00000	5.5086 (5.4796)	0.00	2.165	7
M1*	0.00140	5.5001 (5.4931)	0.00	2.165	2
M2*	0.01184	5.5299 (5.4396)	0.00	2.165	6
M3*	0.02115	5.5378 (5.4237)	0.00	2.170	1
M4*	0.03008	5.5055 (5.4740)	0.00	2.180	1
M5*	0.03008	5.5012 (5.4774)	0.00	2.180	2
M6*	0.05879	5.4690 (5.5103)	-0.04	2.240	1

configuration parameters and one has to be careful to calculate the true ground state properties and avoid assigning one of the meta-stable states as the GS.

The occupation-matrix control, simulated-annealing, and U-ramping methods, which have been introduced by other researchers, may help one to find lower-energy states but no guarantee to be the lowest-energy state, i. e., the "true" ground state (GS). In this work, a new simple and straight-forward method of SMC was introduced which helps to find the "true" GS as well as

the meta-stable states of 1k-order AFM UO_2. It was shown that the GS of this system is achieved when the spin-symmetry of the oxygen atoms was broken. The SMC method was applied in the context of two "all-equivalent oxygen atoms" and "two-inequivalent oxygen atoms" models for the initial magnetizations of the U1 and U2 atoms set to +0.5 and -0.5, respectively. In both calculations, the results showed that the GS is obtained for asymmetric values of O-atom starting magnetizations. In the first model, 7 doubly-degenerate

states were predicted, while in the second model, 17 different states, including the GS, were predicted. The GS's in the two models showed the same geometric and energetic properties. The DOS's and PDOS's for different states in the simplified model were compared and the comparison showed that the GS, M1, and M2 states are insulators, while the M3 has metallic behavior. Moreover, it was shown that the *5f* orbitals of the U-atoms have the strongest contribution to the density of states of both valence and conduction bands. To visualize the amount of asymmetry in the $n_\uparrow$ and $n_\downarrow$ electron densities for the GS and meta-stable states, we have plotted the electronic polarization densities on the three different *z* planes in the unit cell. The plots for the planes containing O-atoms showed different behaviors for all states. The three states of GS, M1, and M2 showed similar behaviors on the z_3 plane. To check the

sensitivity of the energetic and geometric properties of the GS and meta-stable states on the values of the initial magnetizations ± 0.5 for the U1 and U2 uranium atoms in the 1k-order AFM configuration, we have changed these starting magnetizations of U1 and U2 atoms to +1.0 and -1.0 respectively, and recalculated the simplified all-equivalent oxygen atoms model. The results showed that the energetic and geometric behaviors of the meta-stable states strongly depend on the initial magnetizations of the U-atoms, and the degeneracies in the meta-stable states are also dependent on the choice of initial magnetization of U-atoms. The most important result was that the GS properties were unique in the models employed. Finally, using the GGA-PBEsol approximation for the XC functional, we have obtained electronic and geometric properties of the GS in excellent agreement with experimental values.

References

1. G Amoretti, *et al.*, *Phys. Rev.* B **40** (1989) 1856.
2. J Faber, G H Lander, and B R Cooper, *Phys. Rev. Lett.* **35** (1975) 1770.
3. A Kokalj and *J. Mol. Graph. Model.* **17** (1999) 176.
4. M Idiri, *et al.*, *J. Phys. Rev*. B **70** (2004) 014113.
5. Y Baer and J Schoenes, *Solid State Commun*. **33** (1980) 885.
6. J Schoenes, *J. Appl. Phys.* **49** (1978) 1463.
7. V A Gubanov, and A Rosen, and D E Ellis, *Solid State Commun.* **22** (1977) 219.
8. S L Dudarev, *et al.*, *Phys. status solidi* (a) **166** (1998) 429.
9. J Schoenes, *Phys. Rep.* **63** (1980) 301.
10. S L Dudarev, *et al., Philos. Mag*. B **75** (1997) 613.
11. B Dorado, *et al., Phys. Rev*. B **79** (2009) 235125.
12. J Pegg, *et al., J. Nucl. Material.* **492** (2017) 269.
13. S Sheykhi and M Payami, *Phys.* C*: Supercond. Appl.* **549** (2018) 93.
14. M S Christian, E R Johnson, and T M Besmann, *J. Phys. Chem.* A **125** (2021) 2791.
15. P Hohenberg and W Kohn, *Phys. Rev*. **136** (1964) B864.
16. W Kohn, and L J Sham, *Phys. Rev*. **140** (1965) A1133.
17. M Cococcioni, and S De Gironcoli, *Phys. Rev*. B **71** (2005) 035105.
18. B Himmetoglu, *et al.*, *Int. J. Quant. Chem.* **114** (2014) 14.
19. M Freyss, *et. al.,* "*Scientific Highlight of the Month*". (2012).
20. J P Allen and G W Watson, *Phys. Chem. Chem. Phys.* **16** (2014) 21016.
21. H Y Geng, *et al.*, *Phys. Rev*. B **82** (2010) 094106.
22. B Meredig, *et al.*, *Phys. Rev*. B **82** (2010) 195128.
23. J P Perdew, *et al.; Phys. Rev. Lett*. **100** (2008) 136406; Erratum: *Phys. Rev. Lett.* **102** (2009) 039902.
24. P Giannozzi *et al.; J. Phys. Condens. Matter* **21** (2009) 395502.
25. P Giannozzi, *et al., J. Chem. Phys*. **152** (2020) 154105.
26. A Dal Corso, *Comput. Mater. Sci*. **95** (2014) 337.
27. D D Koelling and B N Harmon, *J. Phys*. C: *Solid State Phys*. **10** (1977) 3107.
28. M Payami and S Sheykhi, *arXiv:2209.00724*.
29. M P A T Methfessel and A T Paxton, *Phys. Rev*. B **40** (1989) 3616.
30. P E Blochl, O Jepsen, and O K Andersen, *Phys. Rev*. B **49** (1994) 16223.
31. T Yamazaki and A Kotani, *J. Phys. Soc. Japan* **60** (1991) 49.
32. A Kotani and T Yamazaki, *Prog. Theor. Phys. Supp.* **108** (1992) 117.
33. Y Hinuma *et al., Comput. Mater. Sci.* **128** (2017) 140.
34. A Togo and I Tanaka, *arXiv:1808.01590* (2018).
35. E Ratcliff, Laura *et al*., *J. Phys.: Condens. Matter* **34** (2022) 094003